Structural Characterization of Co·Bleomycin A2 Brown: Free and Bound to d(CCAGG*C*CTGG)

**Siu Man Lui,† Dana E. Vanderwall,‡ Wei Wu,† Xue-Jun Tang,§
Christopher J. Turner,‖ John W. Kozarich,*,‡ and JoAnne Stubbe*,†**

*Contribution from the Departments of Chemistry and Biology and Francis Bitter Magnet
Laboratory, Massachusetts Institute of Technology, Cambridge, Massachusetts 02139,
Merck Research Laboratory, P.O. Box 2000, Rathway, New Jersey 07065-0900, and
Wyeth-Ayerst Research, 401 North Middletown Road, Pearl River, New York 10965*

Abstract: A model for the structure of the aquated form of cobalt bleomycin (H$_2$O-CoBLM or CoBLM A2 brown), free and bound to d(CCAGG*C*CTGG)$_2$ (**1**) is reported based on molecular modeling using the constraints obtained from 2D NMR studies. CoBLM A2 brown has a chiral organization of its ligands, including the axial primary amine of β-aminoalanine, identical to the hydroperoxide form of cobalt BLM (HOO-CoBLM or CoBLM A2 green). H$_2$O-CoBLM forms a 1:1 complex with **1** with a K_d of 2×10^{-6} M which is in slow exchange on the NMR time scale. The complex exhibits 44 intermolecular NOEs and 56 intramolecular NOEs within H$_2$O-CoBLM itself. Molecular modeling reveals that H$_2$O-CoBLM's mode of binding, basis for sequence specificity, and chemical specificity are almost identical to that previously reported for HOO-CoBLM (Wu, W.; Vanderwall, D. E.; Turner, C. J.; Kozarich, J. W.; Stubbe, J. *J. Am. Chem. Soc.* **1996**, *118*, 1281–1294). The bithiazole tail is inserted from the minor groove 3′ to *C*6 and the terminal thiazolium ring is well stacked between the bases G14 and G15, while the penultimate thiazolium ring is only partially stacked between the bases of *C*6 and C7. The basis for sequence specificity involves hydrogen-bonding interactions between the 4-amino group and N3 of the pyrimidine of BLM and the N3 and 2-amino group of G5 of DNA, forming an unusual base triple. Molecular modeling further reveals that the oxygen of the axial H$_2$O ligand is 2.7 Å from the 4′ H of *C*6, the site of cleavage of iron BLM and light-activated cleavage by HOO-CoBLM. Preliminary studies of H$_2$O-CoBLM with d(CCAGTACTGG) (**4**) and d(GGAAGCTTCC) (**2**) are also reported.

Introduction

The bleomycins (BLMs, Figure 1) are antitumor antibiotics used clinically in the treatment of a variety of cancers.[1] Their cytotoxicity is thought to be related to their ability, in the presence of the required iron and O$_2$ cofactors,[2,3] to degrade duplex DNA, RNA, and/or DNA–RNA hybrids.[4–9] The cleavage of DNA is sequence and site specific, occurring at *Py* in d(Gp*Py*) sequences and being initiated by 4′ hydrogen
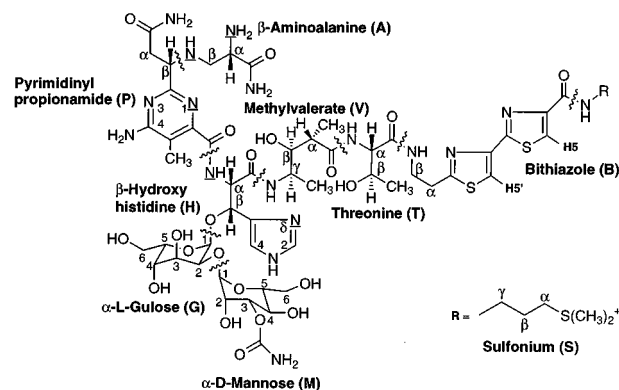

Figure 1. Structure of bleomycin A2. Ns are the ligands that are coordinated to the essential metal cofactor; V and T represent the peptide linker connecting the metal-binding domain (A, P, H) and the DNA-binding domain that includes the bithiazole rings (B) and the sulfonium tail (S).

abstraction.[6,10–12] Recently, the first insight into the basis of these specificities was revealed by 2D NMR analysis of CoBLM A2 green bound to d(CCAGGCCTGG)$_2$ (**1**)[5,13–15] and preliminary results with d(GGAAGCTTCC)$_2$ (**2**) and d(AAACGTTT)$_2$ (**3**).[16,17]

* Authors to whom correspondence should be addressed.
† Departments of Chemistry and Biology, Massachusetts Institute of Technology.
‡ Merck Research Laboratory.
‖ Wyeth-Ayerst Research.
‖ Francis Bitter Magnet Laboratory, Massachusetts Institute of Technology.
⊗ Abstract published in *Advance ACS Abstracts,* September 15, 1997.

(1) (a) Sikic, B. I., Rozencweig, M., Carter, S. K., Eds. *Bleomycin Chemotherapy*; Academic Press: Orlando, FL, 1985. (b) Umezawa, H. *Anticancer agents based on natural product models*; Academic Press, Inc.: 1980; pp 147–166. (c) Lazo, J. S.; Sebi, S. M.; Schellens, J. H. *Cancer Chemother. Biol. Response Modif.* **1996**, *16*, 39–47. (d) Mir, L. M.; Tounekti, O.; Orlowski, S. *Gen. Pharmacol.* **1996**, *27*, 745–748. (e) Hecht, S. M. *Summary of the bleomycin symposium*; Springer-Verlag: New York, 1979.
(2) Sausville, E. A.; Peisach, J.; Horwitz, S. B. *Biochemistry* **1978**, *17*, 2740–2746.
(3) Sausville, E. A.; Peisach, J.; Horwitz, S. B. *Biochem. Biophys. Res. Commun.* **1976**, *73*, 814–822.
(4) Magliozzo, R. S.; Peisach, J.; Ciriolo, M. R. *Mol. Pharmacol.* **1989**, *35*, 428–432.
(5) Stubbe, J.; Kozarich, J. W.; Wu, W.; Vanderwall, D. E. *Acc. Chem. Res.* **1996**, *29*, 322–330.
(6) Stubbe, J.; Kozarich, J. W. *Chem. Rev.* **1987**, *87*, 1107–1136.
(7) Hecht, S. M. *Acc. Chem. Res.* **1986**, *19*, 383–391.
(8) Kane, S. A.; Hecht, S. M.; Sun, J.-S.; Garestier, T.; Héléne, C. *Biochemistry* **1995**, *34*, 16715–16724.
(9) Hecht, S. M. *Bioconjugate Chem.* **1994**, *5*, 513–526.

(10) Giloni, L.; Takeshita, M.; Johnson, F.; Iden, C.; Grollman, A. P. *J. Biol. Chem.* **1981**, *256*, 8608–8615.
(11) Rabow, L. E.; McGall, G. H.; Stubbe, J.; Kozarich, J. W. *J. Am. Chem. Soc.* **1990**, *112*, 3203–3208.
(12) Rabow, L. E.; Stubbe, J.; Kozarich, J. W. *J. Am. Chem. Soc.* **1990**, *112*, 3196–3203.

CoBLM A2 green (HOO-CoBLM) has an octahedral coordination environment (Figure 1, N indicate ligands) with the primary amine of β-aminoalanine and a hydroperoxide as the axial ligands. This complex cleaves DNA only in the presence of light and does so with the same sequence and chemical specificity as the FeBLMs.[18−21] These similarities, its diamagnetic character, and exchange inert ligands made it the metallo-BLM of choice for investigation by 2D NMR methods.[13−16,22−24] Most importantly, CoBLM A2 green is believed to be an excellent analog of the activated BLM, HOO-FeBLM, and thus the model structure obtained with this form of metallo-BLM is thought to be indicative of the FeBLM system.[5,25,26] During the synthesis of HOO-CoBLM, CoBLM A2 brown, with an axial H_2O or HO^- ligand, is also generated.[27−29] It is also diamagnetic, and its H_2O or HO^- axial ligand is exchangeable with solvent.[27] In contrast to HOO-CoBLM, it does not catalyze cleavage of DNA.[21]

In previous studies of Xu et al. on a mixture of CoBLM A2 green and brown forms, the latter was proposed to have a different ligand organization relative to the former.[23] This postulate was based on 2D NMR studies which revealed differences between these compounds in observed NOEs from their peptide linker region (Figure 1) and bithiazole tail to their metal-binding domain (Figure 1).[23] More recently, this postulate was reinforced by NMR studies of each of these BLM analogs with oligonucleotides 2 and 3.[16] Mao et al. observed that the green form is in slow exchange with 2 and 3 on the NMR time scale and that the brown form is in fast exchange. These observations were taken as evidence of alternative binding modes for these species and as additional evidence in support of an alternative screw sense for the brown form, relative to the green form.[16] Their preliminary studies have prompted us to report our successful efforts to determine, by 2D NMR methods, a model of the structure of CoBLM A2 brown and its complex with 1. In contrast to the proposal of Petering and co-workers,[16,23] CoBLM A2 brown is shown to bind to 1 in almost identical fashion to the corresponding green form. Thus, the brown and green forms have identical ligand organization

around the metal. In addition, preliminary studies with the brown form and oligonucleotides 2 and d(CCAGTACTGG)₂ (4) suggest that the brown form, consistent with its lower binding affinity than the green form, can exhibit altered binding dynamics and multiple modes of binding. The basis for the similarities and differences between the brown and green forms of CoBLM A2 will be discussed.

Experimental Section

Sample Preparation. CoBLM A2 brown and decameric oligonucleotides 1, 2, and 4 were synthesized and purified as previously described.[15] The acetate of the HPLC elution buffer in the CoBLM A2 brown sample was removed by repeated lyophilization. The cobalt content in A2 brown was measured by the Chemical Analysis Laboratory, the University of Georgia, Athens, GA, using inductively coupled plasma emission spectroscopy. The extinction coefficient was determined to be $2.05 \pm 0.2 \times 10^4$ M^{-1} cm^{-1} at 290 nm. The electrospray mass spectrum was obtained as previously described.[14]

Binding Studies of CoBLM A2 Brown with 1. The binding parameters were obtained from fluorescence quenching measurements as previously described.[20,30] Fluorescence spectra of CoBLM A2 brown were recorded using a Perkin-Elmer Fluorometer (LS 50) at 20 °C. Titrations were carried out by the addition of a fixed amount of DNA (~3 μM) to variable amounts of CoBLM A2 brown (2−10 μM) in 50 mM sodium phosphate at pH 6.8. Conditions were chosen so that each set of experiments covered as wide a range of percent bound CoBLM as practical. In all experiments, the fluorescence readings were corrected by subtracting the background fluorescence of DNA.

NMR Experiments. The procedures employed were similar to those previously described.[14,15] All NMR experiments were performed on either a 750 MHz Varian NMR spectrometer or a 600 or 500 MHz custom-built instrument at the MIT Francis Bitter Magnet Laboratory. The program Felix (version 2.3, Molecular Simulations Inc., formally, Biosym Technologies, Inc.) running on a Silicon Graphics work station was used to process the NMR data. ^1H and ^{13}C chemical shifts were referenced to an internal standard, sodium 3-(trimethylsilyl)-1-propanesulfonate at 0.00 ppm. A typical NMR sample containing 2−3 mM complex in 50 mM sodium phosphate (pH 6.8) was prepared by titrating the DNA sample with CoBLM A2 brown. For experiments in D_2O, the complex sample was lyophilized four times from 99.9% D_2O and then dissolved in 99.996% D_2O. For experiments in H_2O, the complex was dissolved in 90% H_2O/10% D_2O.

DQF-COSY, TOCSY (Z-filtered TOWNY or DIPSI-2 isotropic mixing sequence with 35, 70, and 140 ms mixing times),[31] and NOESY (100, 200, and 400 ms mixing times) experiments were recorded at 20 °C in D_2O or H_2O. Data sets with 4096 × 512 complex points were acquired with sweep widths of 5500 (500 MHz instrument) or 8000 Hz (750 MHz instrument) in both dimensions and 32 scans per t_1 increment. During the relaxation delay period, a 2.0 s presaturation pulse was used for solvent suppression. For the NOESY experiments in H_2O, a Watergate pulse sequence[32] was used, and data sets with 4096 × 512 complex points were acquired with sweep widths of 12 000 Hz (600 MHz instrument) in both dimensions. The t_1 dimension was zero-filled to 4096 data points, and spectra were processed with a combination of exponential and Gaussian weighting functions. In all cases, ridges in t_1 were reduced by multiplying the first point in t_1 by half prior to the Fourier transformation. Baselines were corrected with a polynomial or an automatic baseline correction routine in t_2 when necessary.

Molecular Modeling. BLM A2 was constructed as previously described[14,15] but with a H_2O or HO^- as the axial ligand. The bond

(13) Wu, W.; Vanderwall, D. E.; Stubbe, J.; Kozarich, J. W.; Turner, C. J. *J. Am. Chem. Soc.* **1994**, *116*, 10843−10844.

(14) Wu, W.; Vanderwall, D. E.; Lui, S. M.; Tang, X.-J.; Turner, C. J.; Kozarich, J. W.; Stubbe, J. *J. Am. Chem. Soc.* **1996**, *118*, 1268−1280.

(15) Wu, W.; Vanderwall, D. E.; Turner, C. J.; Kozarich, J. W.; Stubbe, J. *J. Am. Chem. Soc.* **1996**, *118*, 1281−1294.

(16) Mao, Q.; Fulmer, P.; Li, W.; DeRose, E. F.; Petering, D. H. *J. Biol. Chem.* **1996**, *271*, 6185−6191.

(17) Petering, D. H.; Mao, Q.; Li, W.; DeRose, E.; Antholine, W. E. *Met. Ions Biol. Syst.* **1996**, *33*, 619−648.

(18) Chang, C.-H.; Meares, C. F. *Biochemistry* **1982**, *21*, 6332−6334.

(19) Worth Jr., L.; Frank, B. L.; Christner, D. F.; Absalon, M. J.; Stubbe, J.; Kozarich, J. W. *Biochemistry* **1993**, *32*, 2601−2609.

(20) Chang, C.-H.; Meares, C. F. *Biochemistry* **1984**, *23*, 2268−2274.

(21) Saito, I.; Morii, T.; Sugiyama, H.; Matsura, T.; Meares, C. F.; Hecht, S. M. *J. Am. Chem. Soc.* **1989**, *111*, 2307−2308.

(22) Wu, W.; Vanderwall, D. E.; Teramoto, S.; Lui, S.-M.; Hoehn, S.; Tang, X.-J.; Turner, C. J.; Kozarich, J. W.; Boger, D. L.; Stubbe, J. *Nucleic Acids Res.*, submitted.

(23) Xu, R. X.; Nettesheim, D.; Otvos, J. D.; Petering, D. H. *Biochemistry* **1994**, *33*, 907−916.

(24) Vanderwall, D. E.; Lui, S.-M.; Wu, W.; Tang, X.-J.; Turner, C. J.; Kozarich, J. W.; Stubbe, J. *Chem. Biol.* **1997**, *4*, 373−378.

(25) (a) Burger, R. M.; Peisach, J.; Horwitz, S. B. *J. Biol. Chem.* **1981**, *256*, 11636−11644. (b) Burger, R. M.; Peisach, J.; Horwitz, S. B. *J. Biol. Chem.* **1982**, *257*, 3372−3375. (c) Burger, R. M.; Kent, T. A.; Horwitz, S. B.; Münck, E.; Peisach, J. *J. Biol. Chem.* **1983**, *258*, 1559−1564.

(26) Sam, J. W.; Tang, X.; Peisach, J. *J. Am. Chem. Soc.* **1994**, *116*, 5250−5256.

(27) Chang, C.-H.; Dallas, J. L.; Meares, C. F. *Biochem. Biophys. Res. Commun.* **1983**, *110*, 959−966.

(28) Xu, R. X.; Antholine, W. E.; Petering, D. H. *J. Biol. Chem.* **1992**, *267*, 944−949.

(29) Xu, R. X.; Antholine, W. E.; Petering, D. H. *J. Biol. Chem.* **1992**, *267*, 950−955.

(30) Chien, M.; Grollman, A. P.; Horwitz, S. B. *Biochemistry* **1977**, *16*, 3641−3647.

(31) (a) Kadkhodaei, M. K.; Hwang, T.-L.; Tang, J.; Shaka, A. J. *J. Magn. Reson. Ser. A* **1993**, *105*, 104−107. (b) Rance, M. *J. Mag. Reson.* **1987**, *74*, 557−564. (c) Shaka, A. J.; Lee, C. J.; Pines, A. *J. Mag. Reson.* **1988**, *77*, 274−293.

(32) Sklenar, V.; Piotto, M.; Leppik, R.; Saudek, V. *J. Magn. Reson. Ser. A* **1993**, *102*, 241−245.

length for Co$-$O (H_2O or HO^-) was set at 1.945 Å.[33] The charges for the CoBLM A2 brown were determined using the template method of Quanta by assuming a total charge of $+2$ (HO^-) or $+3$ (H_2O) and smoothing over all atoms.

All calculations were carried out with Quanta 4.1/CHARMM 24 (Molecular Simulations Inc.) on a Silicon Graphics Indigo2 or a Cray Y-MP or J-90. The calculation of nonbonded van der Waals and electrostatic interactions were truncated at 13 Å, using a cubic switching function between 8.0 and 12 Å. The distance-dependent dielectric constant algorithm in the CHARMM package was used. The list of nonbonded terms was updated every 20 steps, except in the molecular dynamics run, where the list was updated when any atom moved >0.5 Å. The terms for electrostatic interactions and hydrogen bonds were not included in any calculations with the free CoBLM A2 brown and were only included in the final 15 ps step of the calculations for the CoBLM A2 brown/DNA complex. Hydrogen bonds were cut off at 5.0 Å, and switched between 3.5 and 4.5 Å. Hydrogen bonds were also cut off at 90° and switched between 130 and 110°. The SHAKE algorithm was used to fix all bond lengths to hydrogen atoms.[34] Verlet molecular dynamics calculations were used with a 0.001 ps time step. Following heating, the temperature was maintained by scaling the velocities of the atoms as necessary to keep the temperature at 300 ± 10 K. In the final 15 ps molecular dynamics phase, scaling was only required one or two times. To prevent unrealistic distortion of the structure due to the high temperature employed and the experimental constraints, all force constants for bond distance and angles were set at 1000 kcal mol^{-1} Å^{-2} and 500 kcal mol^{-1} rad^{-2}, respectively, during molecular dynamics. The standard CHARMM potential energy was used for all energy minimizations. Distance constraints were applied using a square well potential, and dihedral constraints were applied using a simple harmonic function.

The DNA was constructed in Quanta in either an A- or a B-form conformation as previously described.[15] The programs NEWHELIX93 (Protein Data Bank) and CURVES were used to measure DNA conformational parameters for DNA. The intramolecular distance constraints used for DNA included 28 restraints between base pairs (1.7$-$2.2 Å) to maintain Watson$-$Crick hydrogen bonding. No other distance constraints were used in the modeling that were not derived from an observed NOESY crosspeak.

Distance and Dihedral Angle Constraints. All NOEs were classified as strong, medium, or weak based on visual inspection of the cross-peak intensities in the 200 ms NOESY spectra. Forty four intramolecular NOEs were used as distance constraints in free CoBLM A2 brown. In its complex with **1**, 56 intraCoBLM NOEs and 44 intermolecular NOEs were used as constraints. In both cases, these constraints were set at 1.9$-$3.0, 1.9$-$4.0, and 1.9$-$5.0 Å for strong, medium, and weak NOEs, respectively. The 206 intramolecular distance constraints for DNA were set at 1.9$-$3.0 Å, 2.5$-$4.0 Å, and 3.5$-$5.0 Å for strong, medium, and weak NOEs, respectively. An additional 1.0 Å was added to the constraints for the pseudoatoms of methyl and ambiguous methylene protons. The analysis of the coupling constants in free CoBLM A2 brown was based on the measurements in 1D spectra collected in D_2O and H_2O. The generalized Karplus equation that considers the electronegativity of substituents[35] was used to derive the dihedral angle constraints in CoBLM A2 brown, as previously described.[14] For CoBLM A2 brown in the complex with **1**, coupling constants were derived from 2D COSY spectra. The respective dihedral angles were qualitatively constrained to a gauche conformation for J coupling values of 0$-$4 Hz and trans conformation for those >8 Hz.

Restrained Molecular Dynamics (MD). For the free CoBLM A2 brown, four different starting structures were constructed using either the primary amine of the β-aminoalanine or the amino group of the

(33) (a) Busch, D. H.; Jackson, P. J.; Kojima, M.; Chmielewski, P.; Matsumoto, N.; Stevens, J. C.; Wu, W.; Nosco, D.; Herron, N.; Ye, N.; Warburton, P. R.; Masarwa, M.; Stephenson, N. A.; Christoph, G.; Alcock, N. W. *Inorg. Chem.* **1994**, *33*, 910$-$923. (b) Hancock, R. D. *Prog. Inorg. Chem.* **1989**, *37*, 187$-$291. (c) Charles, R.; Ganly-Cunningham; Warren, R.; Zimmer, M. *J. Mol. Struct.* **1992**, *265*, 385$-$395.

(34) van Gunsteren, W. F.; Berendsen, H. J. C. *Mol. Phys.* **1977**, *34*, 1311$-$1327.

(35) Haasnoot, C. A. G.; De Leeuw, F. A. A. M.; Altona, C. *Tetrahedron* **1980**, *36*, 2783$-$2792.
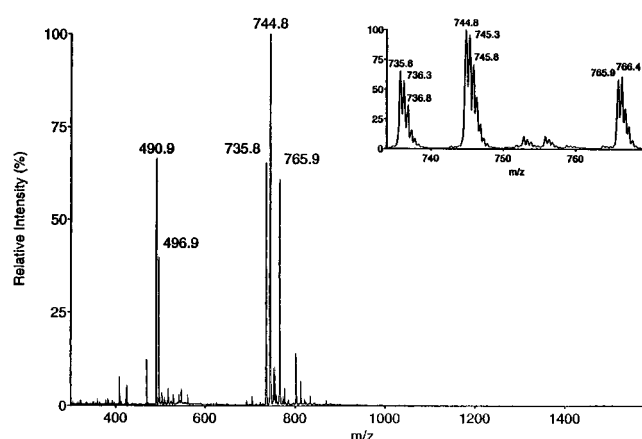
Figure 2. Electrospray mass spectrum of CoBLM A2 brown. The inset shows the isotopic distribution of the peak at *m/z* 735.8, 744.8, and 765.9.

carbamoyl moiety of the mannose as an axial ligand and changing the chiral organization of the complex (See Results and Discussion). The initial structure of the complex between A2 brown and **1** was constructed by manually docking the bithiazole moiety between C6·G15 and C7·G14, followed by energy minimizations as described previously.[15,16] The position of the bithiazole was determined by the NOEs observed between its protons and the DNA. In the case of each of the four free CoBLM A2 brown structures and in the case of the complex with **1**, 20 calculations of restrained MD simulated annealing were run using a protocol identical to that previously described for free CoBLM A2 green and its complex with **1**.[14,15] The protocol consisted of heating the system to 1000 K over 8 ps with no distance constraints in the case of each free CoBLM A2 brown structure or over 6 ps with weak distance constraints in the case of the complex. Then the force constant applied to the distance constraints was gradually increased (6.5 ps), followed by a high-temperature equilibration (10 ps), slow cooling to 300 K (7 ps), gradual introduction of the dihedral angle constraints (10 ps), and a final molecular dynamics stage (15 ps). The final structure for each iteration was generated by averaging the coordinates of the final 5 ps of the 15 ps molecular dynamics simulation, followed by 2000 steps of conjugate gradient minimization with the distance constraints and CoBLM A2 brown dihedral angle constraints. The final average structure was generated by averaging and minimizing the final structures of each iteration and is the model structure used in the figures and for the discussion. In the MD calculations of the CoBLM A2 brown complex with **1**, 10 B-form and 10 A-form DNA structures were initially used. Regardless of the starting DNA conformation, the final averaged structures differed by a rmsd of less than 0.5 Å. Based on this similarity, the final simulated annealing calculations used the B-form model as a starting structure. Calculations carried out with a H_2O ligand or a HO^- ligand in CoBLM A2 brown gave similar results and structures shown below have a H_2O ligand. The distances and angles used to describe the structure are the mean value of all the structures ± 1 standard deviation.

Results and Discussio

Free CoBLM A2 Brown. CoBLM A2 brown was synthesized by a modification of the procedure of Chang et al.[27] and separated from the A2 green, B2 green, and B2 brown forms by HPLC. The extinction coefficient at 290 nm was determined to be 2.05×10^4 M^{-1} cm^{-1}, similar to that of CoBLM A2 green ($\epsilon = 2.1 \times 10^4$ M^{-1} cm^{-1}). CoBLM A2 brown was judged to be $>95\%$ pure on the basis of its 1D NMR spectrum. Its electrospray mass spectrum (Figure 2) was obtained in an effort to identify its sixth ligand. Two clusters of peaks are observed. Within one cluster are peaks with mass-to-charge ratios (*m/z*) of 735.8, 744.8 and 765.9 representing doubly charged species, whereas within the second cluster are peaks with *m/z* of 490.9 and 496.9 representing triply charged species. The isotopic distribution of the doubly charged species can be seen in the

inset of Figure 2 and is consistent with the calculated isotopic distribution. The peaks at m/z of 490.9 and 735.8 have been assigned to $[BLM^+ + Co^{3+} - H^+]^{3+}$ (MW = 490.9 × 3 = 1472.7) and $[BLM^+ + Co^{3+} - 2H^+]^{2+}$ (MW = 735.8 × 2 = 1471.6), respectively, which are in agreement with their respective calculated monoisotopic molecular weights of 1472.44 and 1471.44. The molecular mass of the doubly charged peak at m/z 744.8 is 18 Da higher than the peak at m/z 735.8, which indicates that the sixth ligand is either OH^- $[BLM^+ + Co^{3+} + OH^- - H^+]^{2+}$ or H_2O $[BLM^+ + Co^{3+} + H_2O - 2H^+]^{2+}$. The molecular mass of the triply charged peak at m/z 496.9 is also 18 Da higher than the peak at m/z 490.9, which suggests the sixth ligand is H_2O $[BLM^+ + Co^{3+} + H_2O - H^+]^{3+}$. These conclusions assume that the charge of CoBLM in solution is similar to that observed by electrospray mass spectrometry and the histidine amide is deprotonated. As indicated in Figure 2, the CoBLM A2 brown form has an exceptionally high population of the +3 species at m/z 490.9 and 496.9, ~70% relative to the +2 species. This result is quite different from the green form which has a major population of a +2 species (>90%, m/z of 752.7), consistent with a hydroperoxide ligand.[14] Thus, the electrospray mass spectrometry reveals that the CoBLM A2 brown is probably a heterogeneous mixture of species with a H_2O or an OH^- axial ligand. The peak at m/z 765.9 is assigned to $[BLM^+ + Co^{3+} + CH_3CO_2^- - H^+]^{2+}$, that is, it has $CH_3CO_2^-$ as the sixth ligand. When the volatile buffer used in the HPLC purification of the brown form is not completely removed, H_2O is replaced with the acetate ligand (m/z of 765.9, Figure 2). This observation indicates that the axial ligand in CoBLM A2 brown is not as inert as the hydroperoxide in A2 green. In the NMR experiments described subsequently, the axial ligand was completely exchanged with solvent.

Proton Assignments of Free CoBLM A2 Brown. An essential step in determining the structure of CoBLM A2 brown bound to an oligonucleotide is to define its screw sense and ligation state. The assignment strategy for both exchangeable and nonexchangeable proton resonances is analogous to that previously reported for A2 green. The proton assignments at pH 6.8 and 20 °C (Supporting Information, Table 1) are, in most cases, within 0.1 ppm of those previously reported by Xu et al. at pH 7.4 and 25 °C, for a mixture of A2 green and brown forms.[23] However, the availability of homogeneous A2 brown has allowed the assignment of all the sugar protons. In the case of the A2 green structure, this information was essential for assigning the chirality of the cobalt ligand arrangement.[14]

Previous Model Building Studies. Xu et al. reported the first model for a structure of A2 brown based on their NOE constraints[23] and molecular modeling and arrived at a structure similar to **III** shown in Figure 3. They assumed that the axial ligand was the primary amine of β-aminoalanine in their modeling. The chiral organization of the ligands is the opposite of that for A2 green recently established by Wu et al.[14,15] and favored by Xu et al. from their own studies.[23] Preliminary 2D NMR studies by Mao et al.[16] of homogeneous A2 brown with 1 equiv of d(GGAAGCTTCC)₂ (**2**) failed to detect any intermolecular NOEs between BLM and the DNA, a result differing dramatically from identical studies with A2 green. These results were interpreted by Petering and co-workers to support their proposal that CoBLM A2 brown is of opposite chirality from the corresponding A2 green.[16,23]

Solution Structure of Free CoBLM A2 Brown. In an effort to establish the identity of the second axial amine ligand and the chirality of the free CoBLM A2 brown, molecular dynamics calculations based on NMR constraints were carried out using the two different screw sense isomers with either the primary

amine of β-aminoalanine (**I** and **III**) or the carbamoyl group of mannose (**II** and **IV**) as starting structures (Figure 3, **I**−**IV**). A consensus has been reached regarding the equatorial ligands of CoBLMs, and these are assumed to be identical in all cases considered.[36] By using four starting structures with defined ligands, each possible configuration of the metal-binding region is explicitly considered with respect to the NMR data. This means that determining which structure is most consistent with the data is not dependent on the method used to sample conformational space prior to the application of constraints. The assignment of the chemical shifts of all of the protons (Supporting Information, Table 1) allowed the determination of 44 intramolecular NOEs and their relative strengths (Table 1, comparison of NOEs for the brown and previously reported green form). Use of the 1D NMR spectrum allowed the determination of 12 coupling constants and analysis of these data according to the Karplus relationship allowed the determination of five dihedral angle constraints (Supporting Information, Table 2). Using these constraints and the molecular dynamics calculations described in the Experimental Section and previously described for a similar analysis of CoBLM A2 green,[14] the results for structures **I**−**IV** were obtained (Table 2) and the minimized average structure in each case is shown in Figure 3. As outlined below, the favored structure is **I** (Figure 3) with the primary amine of β-aminoalanine as the axial ligand and a chiral organization of the ligands identical to A2 green.

An analysis of the structures **I**−**IV** has revealed that the screw sense with the axial amine ligand on the upper face (Figure 3, **I** and **II**) is most consistent with the observed NMR data. As previously noted in the case of CoBLM A2 green,[14] **IV**, with the carbamoyl nitrogen as the axial ligand on the same face as the bithiazole can be easily eliminated from further consideration. The extremely large CHARMM potential energy indicates that this structure is highly strained. A significant number of NMR-derived distance constraints are consistently violated, and this structure requires a transconfiguration between the H−CαH and the H−CβH, inconsistent with the small coupling constant observed (2.0 Hz) (Supporting Information, Table 2).

As noted above, **III** has the same screw sense and axial ligation state as the structure proposed by Xu et al. for CoBLM A2 brown.[23] As illustrated in Table 2, this structure does not generally satisfy the constraints as well as the structures of the opposite chirality. More specifically, several NOE distance constraints[37] are consistently violated by 0.1−0.3 Å. While these are not very large errors, they are more numerous and larger than the violations observed in **I**. It should be noted that all but one of these critical NOEs are absent from the data reported by Xu et al.,[23] suggesting that the data used in their calculations may have limited their ability to make a clear distinction between the two possible screw sense isomers of CoBLM brown (**I** vs **III** in Figure 3). In addition, **III** predicts 11 strong or medium NOEs between the α and β protons of the β-aminoalanine and the protons of V and T moieties that are not observed (Table 3 in comparison to Table 1). With the exception of the NOE between A−CαH and H−C2H, none of these NOEs were reported by Xu et al.[23]

It should be noted that previous 2D NMR studies on CO-

(36) (a) Dabrowiak, J. C. *J. Inorg. Chem.* **1980**, *13*, 312−337. (b) Dabrowiak, J. C.; Tsukayama, M. *J. Am. Chem. Soc.* **1981**, *103*, 7543−7550. (c) Dabrowiak, J. C. In *Advances in Inorganic Biochemistry*; Eichhorn, G. L., Marzilli, L. G., Ed.; Elsevier Biomedical: New York, 1982; Vol. 4, pp 69−113.

(37) NOEs, observed intensity: A−CβH to P−CαH, m; P−CβH to T−CβH, w; H−C2H to T−CβH, w; H−C2H to T−CH₃, s; T−NH to V−γCH₃, w.
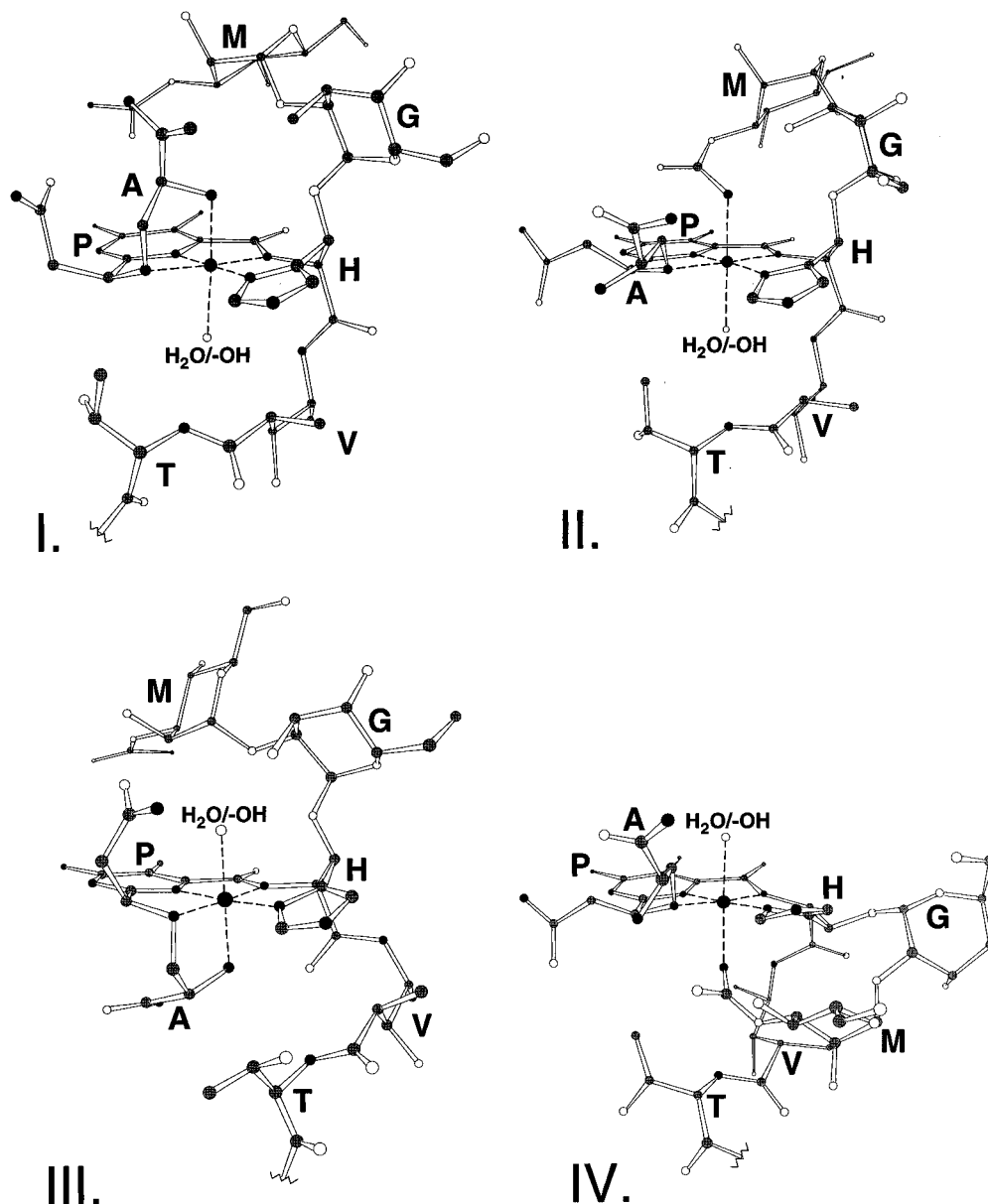
Figure 3. Four possible isomers of CoBLM A2 brown. **I** and **II** have the same screw sense. **I** has the primary amine of A as its axial ligand, while **II** has the carbamoyl nitrogen of M as its axial ligand. **III** and **IV** have the opposite screw sense from **I** and **II**. **III** has the primary amine of A as its axial ligand, while **IV** has the carbamoyl nitrogen of M as its axial ligand. The bithiazole tail including the sulfonium terminus has been excluded for clarity. Structures **I**−**IV** represent the minimized average structures obtained as discussed in the Experimental Section. Carbon, oxygen, and nitrogen atoms are colored gray, white, and black, respectively.

FeBLM and ZnBLM[38,39] have been interpreted to indicate that the carbamoyl group of mannose is an axial ligand to the metal (**II** in Figure 3). This proposal was based on the observation of NOEs between the protons of the mannose moiety (M) and those associated with the metal ligands, H and A. Furthermore, the upfield chemical shift of M−C3H relative to apo-BLM was also cited in support of this hypothesis. A compilation of the chemical shifts of M−C3H for all metallo-BLMs, however, reveals that they all are perturbed by a similar magnitude, even CoBLM A2 green in which the carbamoyl group does not function as an axial ligand.[14] Thus, this shift is not a good criterion for the ligation state. In the present study with CoBLM A2 brown, no NOE cross peaks are observed between the mannose moiety and the metal-binding region (Table 1). These

results provide evidence that mannose is not restricted to the coordination sphere of cobalt and therefore its carbamoyl nitrogen is unlikely to be a ligand. Thus, **II** (Figure 3) appears to be unlikely as well.

Finally, the strongest evidence in support of **I**, as described later, comes from the observation that CoBLM A2 brown binds to **1** in a fashion similar to that proposed for the A2 green with the same oligonucleotide. Neither **III** or **IV** can interact with **1** to satisfy the intermolecular NOEs observed between the drug and DNA. Thus, on the basis of analysis of the NOEs and modeling studies, we favor structure **I** with the primary amine as the axial ligand in CoBLM A2 brown.

Structural Comparison of the Free Brown and Green Forms of CoBLM A2 and Functional Implications. In contrast to the earlier study by Xu et al.,[23] our gross solution structure of free CoBLM A2 brown is very similar to that reported for A2 green, both with respect to its screw sense and the axial ligation state. A least-squares alignment of one of

(38) Akkerman, M. A. J.; Haasnoot, C. A. G.; Hilbers, C. W. *Eur. J. Biochem.* **1988**, *173*, 211−225.

(39) Akkerman, M. A. J.; Neijman, E. W. J. F.; Wijmenga, S. S.; Hilbers, C. W.; Bermel, W. *J. Am. Chem. Soc.* **1990**, *112*, 7462−7474.

Table 1. Comparison of Nontrivial Intramolecular NOEs in Free CoBLM A2 Brown and Green Forms

	brown[a]	green[b]		brown[a]	green[b]
H−C2H···A−CβH′	m	m	V−αCH₃···V−CβH	m	
H−C2H···A−CβH	w	w	V−NH···V−CβH	m	s
H−C2H···A−NH	w	m	V−NH···V−CαH	m	m
H−C2H···P−CβH	w	w	V−NH···V−γCH₃	m	m
H−C2H···T−CH₃	s	s	T−CαH···T−CH₃	m	m
H−C2H···T−CβH	w	w	T−NH···V−αCH₃	w	w
H−C2H···T−CαH	w	w	T−NH···V−CβH	m	m
H−C2H···T−NH	w	w	T−NH···T−CH₃	w	w
H−C2H···V−CαH	m	m	T−NH···V−CαH	m	m
H−C2H···V−αCH₃	w	w	T−NH···V−γCH₃	m	m
H−C4H···V−CαH	w	w	B−C5H···P−CH₃		m
H−C4H···V−αCH₃	m	m	B−C5′H···V−CβH		m
H−C4H···H−CβH	s	s	B−C5′H···V−γCH₃		m
H−C4H···G−C5H	w	w	B−NH···T−CαH	m	m
H−C4H···G−C6/6′H	w	w	B−NH···T−CβH	w	w
H−CαH···G−C1H	s	s	B−NH···B−CαH	w	w
H−CαH···M−C3H		w	B−NH···B−CαH′	w	w
H−CαH···G−C6H		w	B−NH···T−CH₃	w	w
H−CαH···M−C5H		m	G−C1H···M−C5H		m
H−CβH···G−C1H	s	s	G−C1H···G−C6H	w	w
H−CβH···G−C6H		w	G−C1H···G−C4H	w	w
H−CβH···G−C2H		w	G−C1H···M−C2H		w
A−CβH···P−CαH′	m	m	M−C1H···G−C1H	w	w
P−CβH···A−CβH	w	w	M−C1H···G−C2H	m	s
P−CβH···T−CβH	w	w	M−C1H···G−C3H	m	s
V−αCH₃···V−CγH	s	s	M−C1H···G−C4H	w	w
V−γCH₃···V−CβH	s	s			

[a] This study (200 ms). [b] Reference (200 ms).

Table 2. Structure and Energy Statistics from the Molecular Dynamics Calculations with H₂O-CoBLM

	structure I all structures	structure II all structures	structure III all structures	structure IV all structures
rmsd from distance restraints (Å)	0.001−0.012	0.001−0.016	0.014−0.072	0.106−0.152
total no. of violations	1−4	1−6	4−9	9−16
Σ violations (Å)	0.012−0.113	0.008−0.119	0.169−1.337	1.824−3.162
max violation (Å)	0.007−0.064	0.006−0.108	0.080−0.293	0.492−0.783
potential energy terms[a]				
total	57 ± 7	82 ± 4	81 ± 10	313 ± 43
NOE constraint	0.1 ± 0.1	0.1 ± 0.1	2.2 ± 0.9	29 ± 6
dihedral constraint	0.6 ± 0.2	1.1 ± 0.4	1.6 ± 1.3	14 ± 5
van der Waals	−64 ± 6	−58 ± 4	−57 ± 4	−8.7 ± 12
bond	5.2 ± 0.1	6.7 ± 0.5	5.6 ± 0.9	17 ± 4
angle	55 ± 1	65 ± 5	63 ± 3	160 ± 23
dihedral angle	57 ± 1	66 ± 2	64 ± 5	95 ± 7
improper angle	0.7 ± .01	1.2 ± 0.2	1.1 ± 0.5	8.0 ± 2.6
atomic rmsd for heavy atoms of moieties A−T Co, −OH (Å)[b]	0.49−0.88	0.57−0.97	0.49−1.4	0.62−1.2

[a] Mean energy terms in kcal mol^{-1} ± 1 SD. [b] Because of the expected disorder and lack of NOEs to the sulfonium tail, bithiazole, and the sugars, these moieties were not included in the rms calculation.

Table 3. Predicted NOEs from **III** of the Free CoBLM A2 Brown

		rel inten
A−CαH	V−CβH	s
	H−C2H	s
	T−NH	s
	T−CβH	m
	T−CαH	m
	V−CαH	m
	V−NH	m
A−CβH	T−CH3	s/m
	T−CβH	s/m
A−CβH′	T−CβH	m
	T−CH3	m

the low-energy structures of the brown form with the final average structure of CoBLM A2 green results in a rmsd of 0.87 Å. Our modeling results are consistent with the very similar chemical shifts and coupling constants observed for the residues within the metal-binding domain, relative to those previously reported for CoBLM A2 green (Supporting Information, Tables 1 and 2).

A closer examination of A2 brown relative to A2 green reveals that while parts of its linker (V up to T−NH) is folded as observed in A2 green, there is considerably more flexibility from T−NH to the C-terminal end of A2 brown (Figure 4), not observed with A2 green. The folding of the peptide linker region (Figure 1) as well as its flexibility are apparent from several observations. The upfield shifts of V−CαH (1.17 ppm) and V−αCH₃ (0.73 ppm) relative to apo-BLM (2.45 and 1.10 ppm, respectively) suggest a conformation that positions these protons such that they are shielded by the imidazole ring of the β-hydroxyhistidine moiety (**I** in Figure 3). Furthermore, the large downfield chemical shifts of V−NH and T−NH as in the case of A2 green, which are within hydrogen-bonding distance to the penultimate oxygen of the hydroperoxide ligand,[14] suggest a similar hydrogen-bonding interaction between the axial H₂O/OH⁻ ligand of A2 brown and T−NH and V−NH. This arrangement also requires that the linker region is positioned under the metal-binding domain. On the other hand, examination of the coupling constants of V and T (Supporting Informa-
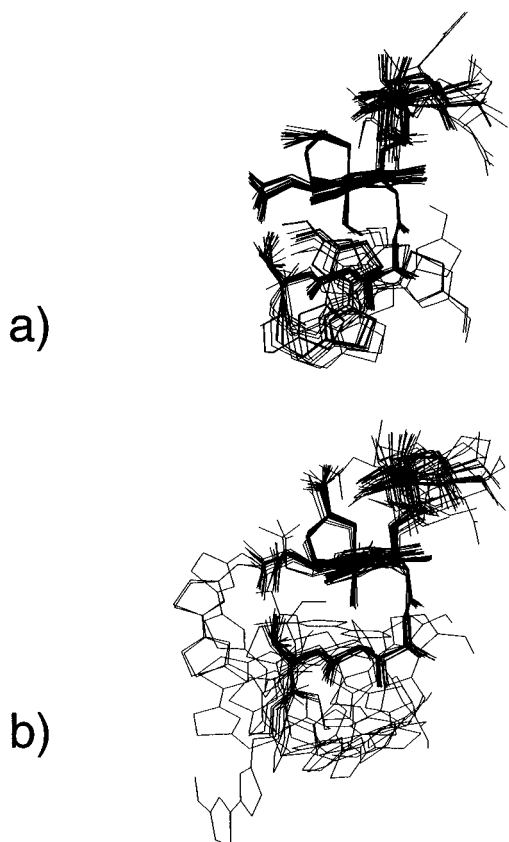
Figure 4. Ensemble of 20 calculated structures of free CoBLM A2 green (a) and free CoBLM A2 brown (b; see also **I** in Figure 3). The sulfonium moiety is excluded for clarity.

Table 4. Intermolecular NOEs between CoBLM A2 Brown and **1** in 50 mM NaPi (pH 6.8) at 20 °C

5′ end	Strand 1	BLM residues	BLM residues	Strand 2	3′ end
A3			A-CαH /m	H4′	T18
			A-CαH /s	H5′*[b]	
G4			A-CαH /m	H1′	C17
			A-CβH′ /w		
			A-CβH′ /m	H4′	
			A-CβH /w		
			A-CαH /s		
G5	H4′	P-CH3 /m			C16
		P-NH2(1) /m			
	H1′	P-CH3 /w			
		P-NH2(1) /m			
	H5″	P-NH2(1) /w			
C6	H5″	P-CH3 /s	B-C5H /w	H1′	G15
		V-γCH3 /m	B-C5H /w	H4′	
	H5′	P-CH3 /m	B-C5H′ /m	NH	
		V-γCH3 /m	B-CβH /w		
	H4′	P-CH3 /m	B-C5H /w	H8	
		V-γCH3 /m			
	H1′	P-CH3 /w			
		P-CβH /w			
	H5	B-C5H′ /m			
	NH2	B-C5H′ /m			
C7	H5″	T-CαH /m	B-C5H /m	H1′	G14
	H5′	V-OH /w	B-C5H /s	H2″	
		T-CαH /w	B-C5H /m	H2′	
	H4′	T-CH3 /w	B-C5H /w	H3′	
		T-CαH /m	B-C5H /w	H4′	
		B-NH /m	B-C5H /w	H8	
	H1′	B-CαH′ /w	S-CβH′ /m		
		B-CαH /w	S-CβH /m		
		B-NH /m	S-CγH /m		
T8					
3′ end	Strand 1		S-CH3 /w	H8	A13
				Strand 2	5′ end

[a] P−NH2 (1) and P−NH2 (2) are the hydrogens at 10.49 and 7.34 ppm, respectively. [b] Used the H5′ pseudoatom.

tion, Table 2) relative to A2 green implies mixed rotamer populations only for the brown, suggesting more flexibility within this region. This flexibility is further apparent from the absence of observed NOEs between the bithiazole protons and protons in the metal-binding and/or linker region (namely, B−C5H′ and V−CβH, V−γCH3, and B−C5H and P−CH3). These NOEs were previously detected in the case of A2 green[14,23] and their absence in A2 brown, as first reported by Xu et al,[23] implies conformational flexibility. This additional flexibility of A2 brown relative to green may provide a explanation for the differences in binding to DNA described subsequently.

Binding Parameters of CoBLM A2 Brown with 1. In order to obtain further evidence for our assignment of the chirality of A2 brown, and to understand how the replacement of HOO⁻ by H_2O/OH^- can alter its binding affinity, CoBLM A2 brown has been investigated with d(CCAGGCCTGG) (**1**). **1** was previously shown to contain a single binding site and cleavage site for CoBLM A2 green.[14] While A2 brown is chemically inert,[21] binding analysis by a similar method gave a K_d of 2.0 × 10⁻⁶ M and a single binding site (supporting Figure 1). This value is similar to the $K_d = 6 \times 10^{-6}$ M recently reported by Mao et al.[16] for its interaction with **2** and the $K_d = 2 \times 10^{-6}$ M for generic calf thymus DNA reported by Chang and Meares.[20] This value is at least 10-fold less than the A2 green form ($K_d = 1.7 \times 10^{-7}$ M) to **1** previously determined by the same method.[14]

Titration of CoBLM A2 brown with **1** was examined by 1D NMR spectroscopy (supporting Figure 2), revealing a striking similarity between it and a similar titration with A2 green. The titration reveals that the single A−H8 resonance (8.20 ppm) of palindromic **1** decreases in intensity, and two new resonances at 8.34 (A3−H8) and 8.00 ppm (A13−H8) appear as the 1:1

complex is generated. Similarly, in the upfield region of the NMR spectrum, the CH3 group of T (1.68 ppm) in free DNA disappears and two new methyl resonances at 1.63 (T8) and 1.70 ppm (T18) appear. These new resonances correspond to the CoBLM−DNA complex in which the symmetry has been disrupted.

Assignments of Protons of the CoBLM A2 Brown Bound to 1. The assignments of the protons of the CoBLM A2 brown in complex with **1** (Supporting Information, Table 1) have been made using strategies previously described in detail for the A2 green complex with **1**.[15] Only the assignments of protons of particular interest with unusual chemical shifts are highlighted here.

A key to understanding the binding specificity of the BLMs to the d(GpPy) sequence was revealed in the solution structure of the A2 green complex with **1**, through the detection of an exchangeable proton at 10.36 ppm assigned to one of the two 4-amino protons of the pyrimidine of BLM.[15] The observation of an exchangeable proton at 10.49 ppm with a similar chemical shift, with three intermolecular NOEs to G5 (H5′, H4′, H1′) (Table 4), suggests by analogy that this proton is associated with the 4-amino group of the pyrimidine ring of CoBLM A2 brown (Supporting Information, Table 1). Consistent with this postulate, this proton exhibits a strong NOE to another exchangeable proton at 7.34 ppm, presumably, the second 4-amino proton of the pyrimidine ring. Both 4-amino protons show medium NOEs to the P−CH3 (Table 5). No NOE is observed between the proton at 10.49 ppm and the imino proton of the G5·C16 base pair, excluding the possibility that it is associated with the 2-amino proton of G5. The chemical shifts of these 4-amino protons have not been detected in free CoBLM A2 brown due to their fast exchange rate. The detection of the unusual downfield shifted 4-amino proton at 10.49 ppm (usually found between 7 and 8 ppm) suggests that it interacts with a heteroatom of DNA by hydrogen bonding in a fashion analogous

Table 5. Intramolecular NOEs of CoBLM A2 Brown and Green Bound to **1** in 50 mM NaPi (pH 6.8) at 20 °C[a]

	brown	green		brown	green		brown	green
H−C2H···A−CβH		w	H−CβH···M−C1H	w	w	V−αCH3···T−CH3	m	
H−C2H···A−CβH′	w	w	H−CβH···V−CγH		w	V−CαH···T−CH3	w	
H−C2H···A−NH	m	m	A−CβH···P−CαH′	m	m	V−NH···V−γCH3	s	s
H−C2H···P−CβH	w	w	A−CβH···P−CαH	m	m	V−NH···V−αCH3	m	s
H−C2H···T−CH3	s	m	A−CβH′···P−CαH′	w	w	V−NH···V−CαH	s	s
H−C2H···T−CβH	w	w	A−CβH···P−CβH	m	w	V−OH···V−CαH	w	w
H−C2H···T−CαH	w	w	A−CβH′···P−CβH	m	w	V−OH···V−αCH3	w	w
H−C2H···T−NH	m	w	A−CβH′···P−CαH	m	m	V−OH···V−γCH3	s	s
H−C2H···V−CαH	m	m	A−CαH···P−CαH	w	w	V−OH···V−CβH	s	s
H−C2H···V−αCH3	w	w	A−NH···T−CH3	w	w	T−NH···V−CαH	m	m
H−C2H···V−CβH	w	w	P−CβH···B−CβH	m	w	T−NH···V−NH	m	m
H−C4H···V−CαH	m	w	P−CH3···V−γCH3	w	w	B−NH···T−CαH	m	m
H−C4H···V−αCH3	m	m	P−CH3···P−NH2 (1)	m	m	B−NH···T−CH3	m	m
H−C4H···H−CαH	w	w	P−CH3···P−NH2 (2)	m	m	B−NH···B−CαH	m	m
H−CαH···V−γCH3	w					B−NH···B−CαH′	m	m
H−CαH···V−αCH3	w		V−αCH3···V−CγH	s	s	S−CαH···S−CH3 (1)	w	w
H−CαH···V−CαH	w		V−γCH3···V−CβH	s	s	S−CαH′···S−CH3(1/2)	w	w
H−CαH···G−C1H	w	m	V−αCH3···V−CβH	s	m			
H−CβH···G−C1H	m	s	V−αCH3···V−γCH3	m	m	G−C1H···M−C1H	m	m
H−CβH···V−αCH3	w	w	V−γCH3···V−CαH	m	m			

[a] w, m, s: weak, medium, strong NOE at 200 ms mixing time. P−NH2 (1), 10.49 ppm; P−NH2 (2), 7.34 ppm. S−CH3 (1), 3.00 ppm; S−CH3 (2), 2.97 ppm.

to that previously observed with A2 green.[15] Mao et al. in a preliminary analysis of the interaction of A2 green with **2** also reported an exchangeable proton with a chemical shift of 10.22 ppm and assigned it to one of the two 2-amino protons of guanine, 5′ to the cleavage site in their oligomer, **2**.[16] Their assignment was based on an NOE to this same GC imino proton. We predict that when their proton assignments and structural analysis are complete, this proton will also be attributed to one of the amino protons of the pyrimidine of BLM.

The appearance of the exchangeable hydroperoxide proton at 8.89 ppm in CoBLM A2 green in the DNA complex provided much insight into the juxtaposition of the reactive species (HOO⁻) to the 4′-H of deoxyribose at the cleavage site.[15] The exchangeable H₂O or hydroxide proton in the complex of CoBLM A2 brown with **1** was not detected. Given the chemical shift similarities between the green and brown forms bound to **1**, the absence of a feature at 8.89 ppm provides further support for its previous assignment in the green complex.[15]

Finally, in many small molecules that bind DNA via intercalation, protons stacked between the DNA bases are shielded and thus upfield shifted.[40,41] Large upfield shifts of B−H5 and B−H5′ (Figure 1) have previously been observed with A2 green interacting with both **1** and **4**,[15,24] shown to bind by partial intercalation. With A2 brown, its B−H5 is shifted from 8.26 ppm in the free form to 7.26 ppm in the complex, while its B−H5′ is shifted from 8.14 to 7.20 ppm (supporting Figure 2). These upfield shifts of ∼1 ppm are thus consistent with a partial intercalative mode of binding of the bithiazole tail for A2 brown to **1** as well. This finding is different from the recent report of Mao et al. that CoBLM A2 brown does not bind by intercalation with **2**.[16] Finally, the methylene protons of the B moiety are also upfield shifted by 0.5, 0.6, and 0.8 ppm for B−CαH, B−CαH′, and B−CβH, respectively, relative to free BLM A2 brown (Supporting Information, Table 1). These upfield shifts, as in the case of the bithiazole protons, are shielded due to the stacking with the ring of the C7 base (vide infra).

Assignments of the Protons of the DNA in the Complex. Proton chemical shifts associated with DNA bases and sugars were established by means of DQF-COSY, TOCSY, and

NOESY experiments in H₂O and D₂O (Supporting Information, Table 3) using sequential strategies and methods similar to those previously described for A2 green with **1**.[15] All of the protons of the deoxyriboses could be assigned except for those associated with H5′, H5″ of DNA due to the extensive spectral overlap. In the DQF-COSY spectrum, all H1′ to H2′ cross peaks, except for C6, were indicative of sugars having C2′-endo-like puckers.[42] For C6, the site of cleavage with A2 green, the H1′ to H2″ and H3′ to H4′ cross peaks were readily detected, while the COSY cross peak between H1′ and H2′ was absent. These observations are consistent with C6 having a C3′-endo-like sugar pucker[42] as previously observed in the A2 green complex with **1**.[15]

Evidence for Intercalation of CoBLM A2 Brown with 1: Sequential NOEs in H₂O and D₂O. Since A2 brown is inert to light-mediated DNA strand cleavage, this method cannot be used to identify its cleavage site(s).[21,43] The question can then be raised as to whether the binding mode of A2 brown to DNA is similar to that observed with A2 green. Tables 4 and 5 present the intermolecular NOEs of CoBLM A2 brown complexed with **1** and the intramolecular NOEs within CoBLM A2 brown, respectively. They are very similar to those previously reported for the A2 green complexed to **1**,[15] suggesting a very similar mode of binding.

Binding via intercalation is often readily apparent by examining disruption of imino−imino sequential interactions when spectra are acquired in H₂O. At 20 °C, the CoBLM A2 brown complex displays eight imino resonances, whereas in the free DNA, only four imino protons are observed. The terminal imino resonances are not detected due to exchange broadening. A 2D NOESY spectrum of the imino region is shown in Figure 5, and the expected NOE cross peak between the imino protons of C6·G15 and C7·G14 is absent in the A2 brown complex. In addition, upfield shifts of imino protons of base pairs C6·G15 and C7·G14 from 12.94 to 12.42 ppm and from 12.89 to 11.88 ppm, respectively, are observed. These results indicate that the bithiazole tail intercalates into DNA on the 3′ side of C6.

(40) Addess, K. J.; Gilbert, D. E.; Olsen, R. K.; Feigon, J. *Biochemistry* **1992**, *31*, 339−350.

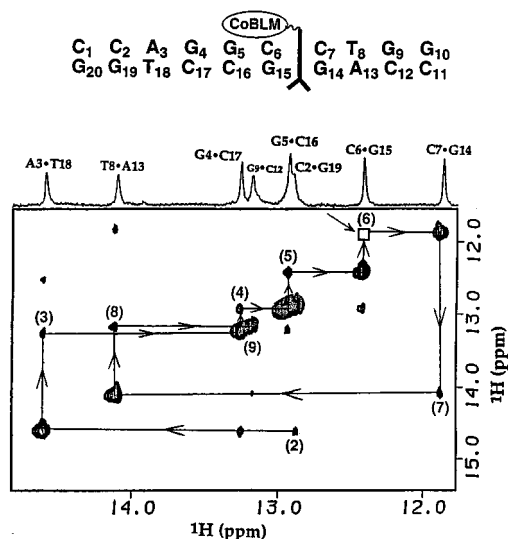(41) Gao, X.; Patel, D. J. *Q. Rev. Biophys.* **1989**, *22*, 93−138.

(42) (a) van Wijk, J.; Huckriede, B. D.; Ippel, J. H.; Altona, C. *Methods Enzymol.* **1992**, *211*, 286−306. (b) Hosur, R. V.; Ravikumar, M.; Chary, K. V. R.; Sheth, A.; Govil, G.; Zu-Kum, T.; Miles, H. T. *FEBS Lett.* **1986**, *205*, 71−76. (c) Majumdar, A.; Hosur, R. V. *Prog. NMR Spectrosc.* **1992**, *24*, 109.

(43) Photolysis of CoBLM A2 brown with **1** reveals cleavage at ∼¹/₁₀₀ that of A2 green. We attribute this to the conversion of the brown to green form that leads to cleavage.[21]

Figure 5. Imino to imino region of the NOESY spectrum (200 ms mixing time, 600 MHz) of a 1:1 complex of CoBLM and **1** in H$_2$O. CoBLM A2 brown and **1** (3.0 mM) in 90% H$_2$O/10% D$_2$O in 50 mM sodium phosphate (pH 6.8) at 20 °C. The sequential imino to imino cross peaks (from second to ninth base pairs) are traced by connecting lines. The missing NOE from the imino proton of G14 to that of G15 is indicated by a box.
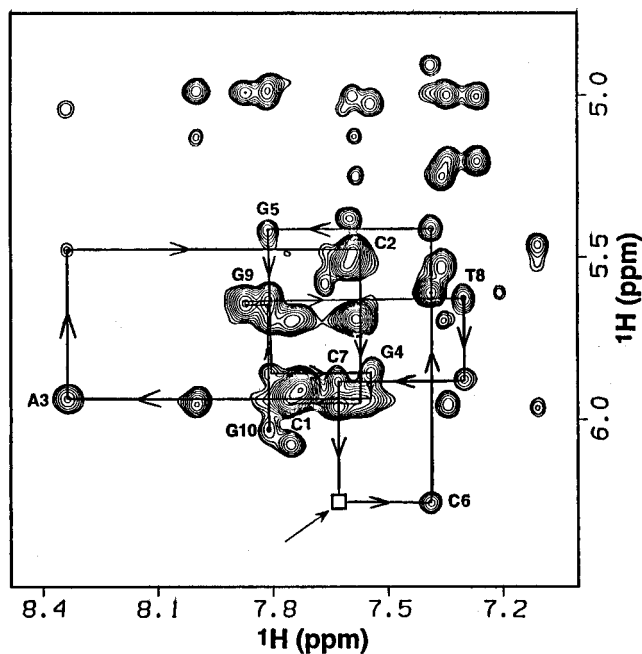

Figure 6. Expanded NOESY spectrum (D$_2$O, 400 ms mixing time, 750 MHz) of the base to sugar H1′ of strand 1 (C1−C2−A3−G4−G5−C6−C7−T8−G9−G10) in the complex. The sequential connectivities are indicated by the connecting lines, and the break is shown by a box at the C6−C7 step.

The normal distance between adjacent base pairs in B-form DNA allows a base proton to interact with the H1′ proton on its neighboring base by through-space coupling and generates a sequential NOE connectivity along a normal undistorted B-form DNA strand.[44] Breaks in the sequential connectivity for both DNA strands of **1** between C7−H6 and C6−H1′ (Figure 6) and G15−H8 and G14−H1′ (data not shown) are observed and also indicate that the bithiazole tail is intercalated between base pairs C6·G15 and C7·G14. Extensive intermo-
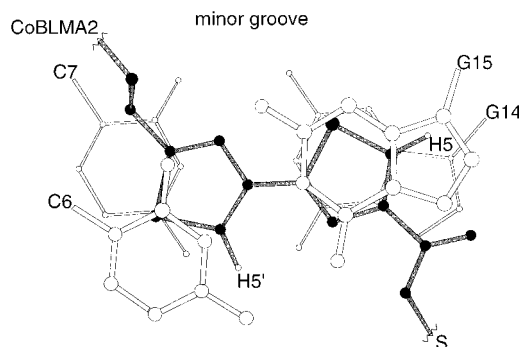

Figure 7. Binding by partial intercalation of the bithiazole tail of CoBLM A2 brown to DNA. A view looking down the helical axis of the final averaged structure showing the terminal thiazolium ring (dark) stacked between the bases of G14 and G15 (white) while the penultimate thiazolium ring (dark) is only partially stacked between the bases of C6 and C7 (white).

lecular NOEs between the bithiazole tail and protons associated with C6, C7, G14, and G15 (Table 4) also support this model.

Molecular Dynamics Studies of CoBLM A2 Brown Bound 1. The data from the 2D NOESY and COSY experiments provided a total of 334 distance constraints and 10 dihedral constraints that could be used to model the structure of CoBLM A2 brown complexed with **1**. Twenty separate molecular dynamics calculations were carried out using a simulated annealing protocol, starting with a different velocity seed each time to avoid bias in the calculations. The resulting structures were in excellent agreement with the NMR data (An overlay of these 20 structures is shown in supporting Figure 3). In the final averaged structures, the rms violation of the distance constraints was 0.007 ± 0.001 Å, with no violations over 0.18 Å. The rms variation of the ensemble of 20 structures from the mean was 0.31−0.59 Å. An overall structure was obtained by averaging 20 calculated structures and was used in the figures shown. The distances and angles used to describe structure are the true mean value of all the structures ±1 standard deviation.

This model structure is very similar to that previously reported for A2 green with **1**, defining a similar basis for binding, DNA sequence specificity, and chemical specificity. The terminal thiazolium ring of CoBLM A2 brown, as shown in Figure 7, is well stacked between base pairs G15 and G14, while the penultimate thiazolium ring is only partially stacked. The DNA is unwound ∼21° over three steps, (G5·C16)−(C6·G15)−(C7·G14)−(T8·A13). The intercalation site is unwound ∼10°, with the preceding step unwound by ∼11°. The bases before and after the intercalation site are buckled, increasing the van der Waals contacts between the drug and DNA. Thus, at the present level of resolution, there are no discernible differences between binding of the bithiazole tail for A2 green and for A2 brown and no specific contacts are detected in either case between this moiety and the DNA.

The basis for the specificity of binding, predominantly the result of the metal- binding domain,[45,46] is shown in Figure 8 and once again is very similar to A2 green.[15] The N3 of the pyrimidine of CoBLM is within hydrogen bond distance to the external proton of the 2-amino group of G5 (2.12 ± 0.03 Å, angle 172 ± 1°). One of the hydrogens of the 4-amino group of this same pyridimine is also within hydrogen bond distance to the N3 of G5 (1.92 ± 0.01 Å, angle 169 ± 2°). The resulting base-triple interaction between G5·C16 and the pyridimine of

(44) Wüthrich, K. *NMR of Proteins and Nucleic Acids*; John Wiley & Sons, Inc: New York, 1986.

(45) Guajardo, R. J.; Hudson, S. E.; Brown, S. J.; Mascharak, P. K. *J. Am. Chem. Soc.* **1993**, *115*, 7971−7977.

(46) Carter, B. J.; Murty, V. S.; Reddy, K. S.; Wang, S.-N.; Hecht, S. M. *J. Biol. Chem.* **1990**, *265*, 4193−4196.
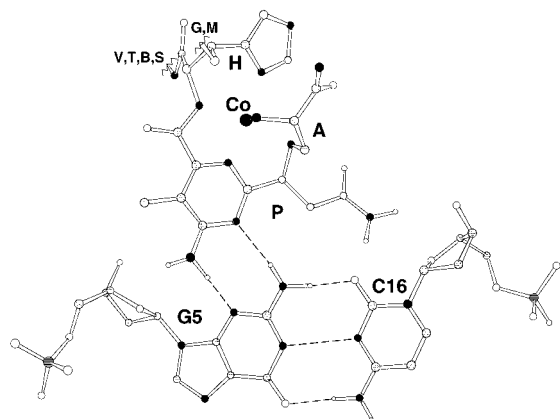
Figure 8. Basis for sequence specificity of DNA cleavage mediated by BLM at d(G-Py) sequences. As shown in the final averaged structure, the P moiety of CoBLM A2 brown forms a minor groove base-triple-like interaction with the G5·C16 base pair. The dotted lines indicate hydrogen bonds between the 4-amino group and N3 of P moiety of CoBLM and N3 and 2-amino group of G5, as well as the Watson−Crick hydrogen bonds. Atoms are colored by element: C, gray; O, white; N, black; P, striped.

CoBLM is very similar to that observed for A2 green.[15] Two potential hydrogen bonds, one between the second proton of the 4-amino group of the Py and the O4′ of deoxyribose of G5 (2.19 ± 0.18 Å, angle 124 ± 8°) and one between the amide proton of the propionamide and O2 of the C16 base (1.84 ± 0.01 Å, angle 176 ± 2°) are also detected in both brown and green complexes. This stable conformation is in contrast with the free brown form in which the propionamide side chain is conformationally flexible (*J* coupling for P−CβH to P−CαH′ is 7.5 Hz in the free form vs <4 Hz in the bound form). The binding to DNA seems to minimize this flexibility.

In the A2 green complex, the determination of the basis for the chemical specificity was assisted by the detection of the hydroperoxide proton, which coupled to modeling suggested that the terminal oxygen of this ligand was 2.28 ± 0.02 Å from the C6−H4′ (Co^{3+} and this 4′-H is 4.57 ± 0.04 Å apart), the site of cleavage.[15] Since the NMR data for A2 brown, coupled to the modeling, reveal that its chirality is identical to A2 green, the only difference between the two is the nature of the axial ligand. In the case of the A2 brown, the hydrogen(s) associated with the axial ligand is(are) not observable due to exchange. Despite the diminished NOE information with A2 brown, molecular modeling without any constraints placed on the distance between the oxygen of the axial H$_2$O/HO$^-$ ligand and the 4′-H of C6 revealed a distance of 2.77 ± 0.17 Å (Co^{3+} and C6−H4′ is 4.09 ± 0.09 Å apart). The juxtaposition of the Co^{3+} to the C6−H4′ proton is readily apparent by its upfield shift of 1.29 ppm relative to the free DNA and a downfield shift of 0.33 ppm for C6 H1′. While the protons in the A2 green complex are also shifted and in the same direction, the magnitude of these shifts is nowhere near as large (0.32 and 0.05 ppm for C6−H4′ and C6−H1′, respectively). The similarities in the distances between the terminal oxygen of the hydroperoxide in A2 green and the only oxygen in A2 brown to C6−H4′, indicate, as we previously concluded, that the resolution of our model is not sufficient to address subtleties of chemical mechanism.

The modeling also reveals that this axial oxygen is within hydrogen bond distance to the NH of the V (2.37 ± 0.26 Å, angle 122 ± 26°) and the NH of the T (2.20 ± 0.12 Å, angle 174 ± 1°) moieties of the linker region. These interactions are analogous to that modeled for A2 green in which the amide

Scheme 1
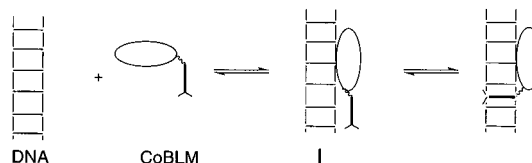
protons of T and V are within H-bonding distance to the penultimate oxygen of the hydroperoxide.[15]

Comparison of the Structures of CoBLMs and Implications in Their Bindings to DNA. One notable difference between the brown and green forms of CoBLM A2 in the absence of DNA (compare parts a and b of Figure 4 is an apparent greater flexibility in the linker region of the brown form. The vicinal coupling constants of V−NH···V−CγH, V−CγH···V−CβH, and T−NH···T−CαH in CoBLM A2 green (7.9, 9.5, and 8.7 Hz, respectively) reflect stable trans conformations. These *J*-coupling values in the CoBLM A2 brown are 6.0, 4.0, and 6.7 Hz, respectively, reflecting either an intermediate conformation between gauche and trans or, alternatively, the averaging of multiple conformations. Because of this ambiguity, no constraints were used on these dihedral angles in the model of CoBLM A2 brown (Supporting Information, Table 2). Nonetheless, the NOE-derived distance constraints (Table 1) have led to a structure for the brown form very similar to that of the green form, suggesting that the average conformation of the linker is nearly the same in these two cobalt complexes.

The question that can be raised then is what distinguishes the binding behavior of these two cobalt derivatives that have K_ds for **1** differing by 10-fold when only their axial ligands (HOO$^-$ vs H$_2$O/OH$^-$) are different. Although the mechanism by which these CoBLM analogs find GpPy sequences that ultimately are cleaved is unknown, the conformational flexibility of peptide linker and bithiazole tail may be a factor in the observed binding differential between the brown and the green forms. Early studies by Povirk and co-workers with CuBLM, using a variety of physical and biochemical methods, suggested a two-step binding model (Scheme 1): a scanning step, followed by a slow intercalation step.[47] Similar mechanisms for the binding of a number of other intercalating agents have been postulated.[48] The conformational difference between A2 green and brown could affect either or both of the postulated steps in the binding process. Thus, the preorganization of the linker and bithiazole tail in the green form could predispose the initial association complex (I) toward intercalation. For the brown complex, the additional entropic cost of organization of the linker and bithiazole moieties for efficient intercalation could result in a significantly reduced equilibrium binding constant relative to the green form. The mechanism(s) of binding of each of these species is(are) under investigation.

Is the Model of Binding of A2 Brown with 1 General? Titration of CoBLM A2 Brown with 2 and 4. The model of A2 brown binding to **1** establishes unambiguously that the chiralities of our CoBLM A2 brown and green forms are identical. The question can then be raised as to whether Mao et

(47) Povirk, L. F.; Hogan, M.; Buechner, M.; N., D. *Biochemistry* **1981**, *20,* 665−671.

(48) (a) Chaires, J. B.; Dattagupta, N.; Crothers, D. M. *Biochemistry* **1985**, *24*, 260−267. (b) Li, H. J.; Crothers, D. M. *J. Mol. Biol.* **1969**, *39,* 461−477. (c) Fox, K. R.; Waring, M. J. *Biochim. Biophys. Acta* **1984**, *802,* 162−168. (d) Fox, K. R.; Brassett, C.; Waring, M. J. *Biochim. Biophy. Acta* **1985**, *840,* 383−392. (e) Fox, K. R.; Wakelin, L. P. G.; Waring, M. J. *Biochemistry* **1981**, *20,* 5768−5779. (f) Dasgupta, D.; Auld, D. S.; Goldberg, I. H. *Biochemistry* **1985**, *24,* 7049−7054. (g) Chen, F.-M. *Biochemsitry* **1988**, *27,* 1843−1848.
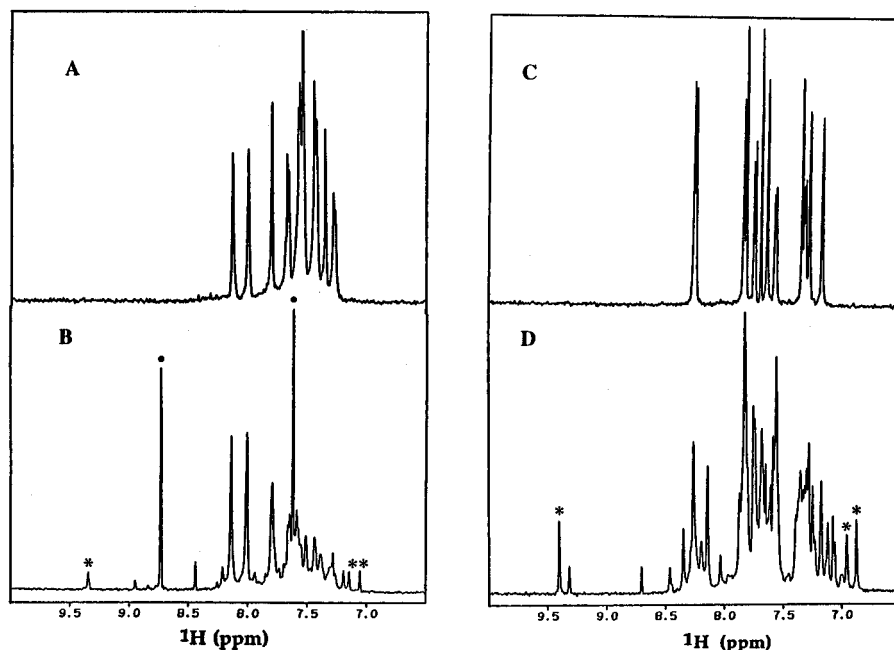
Figure 9. Titration of d(GGAAGCTTCC)₂ (**2**) and d(CCAG*T*ACTGG)₂ (**4**) with CoBLM A2 brown at 20 °C in 50 mM NaPi (pH 6.8): (A) free **2**; (B) 1:1 complex between CoBLM A2 brown and **2**; (C) free **4**; (D) 1:1 complex between CoBLM A2 brown and **4**. The resonances labeled with asterisks and dots are associated with the slow- and fast-exchange complexes respectively.

al. have prepared the opposite screw sense isomer of A2 brown as they originally proposed[16] or whether A2 brown with its weaker binding for DNA relative to A2 green can bind in multiple modes, depending on the sequence context. In order to address this question, CoBLM A2 brown was titrated with **2** and d(CCAGTACTGG)₂ (**4**) and examined by 1D NMR spectroscopy. The results of these titrations are shown in Figure 9. They indicate that A2 brown binds to both **2** and **4** in a fashion more complex than to **1**. The titration with **2** appears similar to that previously reported by Mao et al.,[16] that is, ∼90% of A2 brown appears to be in fast exchange on the NMR time scale. Resonances at 8.70, 7.60, 1.04, 0.91, and 0.85 ppm (compare parts A and B of Figure 9) associated with the A2 brown in fast exchange can be attributed to protons of H−C2H, H−C4H, T−CH₃, V−γCH₃, and V−αCH₃, respectively, based on their assignments in free CoBLM A2 brown (8.67, 7.63, 1.12, 0.92, and 0.73 ppm, respectively). Presumably, the observed chemical shifts are the average of the free and DNA bound forms. In addition to the fast-exchange species, a small portion of A2 brown (∼10%) appears to be in slow exchange, apparent from the protons with the chemical shifts at 9.33, 7.05, and 7.16 ppm (Figure 9B). These chemical shifts can tentatively be assigned to H−C2H, B−C5′H, and B−C5H, respectively, based on their previous assignments in the A2 green complexed with **2**.[16] These results suggest that A2 brown can thus bind to **2** in a mode similar to that of A2 green. Examination of the sequence of **2** suggests that there is a second potential binding site, at the G2A3 step, which may lead to multiple modes of binding. Alternatively, the differences may be attributed to a multistep binding process in which the kinetic constants for CoBLM A2 green and brown differ.

To further address the question of binding specificity of A2 brown, its interaction with **4** was also examined. Our recent studies of A2 green with a stoichiometric amount of **4** demonstrated the formation of two complexes in a ratio of 4:1, both in slow exchange on the NMR time scale.[14] The structure of the predominate species was determined.[24] The titration of

4 with A2 brown reveals multiple complexes as well. However, in this case, as with **2**, the additional complex(es) appear(s) to be in fast exchange. Based on our assignments of A2 green with **4**,[24] protons at 9.40, 6.87, and 6.95 ppm might tentatively be assigned to H−C2H, B−C5′H, and B−C5H, respectively. If these assignments are corrected, they are indicative of an intercalative binding mode of the bithiazole tail. Examination of A2 brown with **1**, **2** and **4** thus reveals in each case a mode of binding analogous to A2 green, but additional modes of binding are observed as well.

Summary

Studies of CoBLM A2 brown with designed oligonucleotides **1**, **2**, and **4** have revealed that it possesses a chiral organization of its ligands identical to A2 green. These studies have further suggested that the conformations of the peptide linker and bithiazole tail play a key role in the mechanism(s) of binding and that a detailed analysis of these mechanism(s) is essential to understanding the difference in the behavior of the metallo-BLMs.

Supporting Information Available: Table of proton chemical shifts (CoBLM A2 brown and **1**) and coupling constants (free and bound CoBLM A2 brown) and figures of fluorescence studies of CoBLM A2 brown with **1**, titration spectra of CoBLM A2 brown with **1**, and overlay of CoBLM A2 brown bound to **1** (6 pages). This material is contained in many libraries on microfiche, immediately follows this article in the microfilm version of the journal, can be ordered from the ACS, and can be downloaded from the Internet; see any current masthead page for ordering information and Internet instructions.